# Fluorescence enhancement by a photonic crystal with a nanorod-structured high index layer

Wei Zhang[1,3] and Brian T. Cunningham[2,3,a)]
[1]*Department of Materials Science and Engineering, University of Illinois at Urbana-Champaign, 1304 West Green Street, Urbana, Illinois 61801, USA*
[2]*Department of Electrical and Computer Engineering, University of Illinois at Urbana-Champaign, 1406 West Green Street, Urbana, Illinois 61801, USA*
[3]*Micro and Nanotechnology Laboratory, University of Illinois at Urbana-Champaign, 208 North Wright Street, Urbana, Illinois 61801, USA*

(Received 8 August 2008; accepted 13 September 2008; published online 2 October 2008)

We report the design and characterization of a one-dimensional photonic crystal slab incorporating a nanorod-structured $TiO_2$ high index layer. The photonic crystal is designed to function as an optical resonator at the wavelength of a laser used to excite fluorescence emission and the highly porous $TiO_2$ film, not only increases the surface area of the device but more importantly allows fluorophores to penetrate into the most intense region of the resonance-enhanced near electric fields. The design shows an enhancement of 193-fold in fluorescence intensity for the detection of cyanine 5-labeled streptavidin in comparison to an unpatterned glass slide. © *2008 American Institute of Physics*. [DOI: 10.1063/1.2994696]

There is a growing interest in designing optically active structures to enhance the output of fluorophores for a wide range of applications including DNA expression analysis and assays for detection of protein biomarkers within bodily fluids. In such applications, the signal-to-noise ratio for detection of fluorescent-tagged analytes at low concentrations may be improved when the assay is performed on an active surface that serves to more efficiently excite fluorophores in comparison to a passive surface. Many structures developed for this purpose utilize the enhanced near fields of metallic surfaces when the plasmonic resonance conditions are fulfilled.[1,2] Since the intensity of emission from fluorophores is proportional to the local electric-field intensity ($E^2$), it is advantageous to place the fluorophores in proximity to the regions where $E^2$ approaches a maximum. In the case of metal nanostructures, typically the maximum field is located at the metal surface and decays exponentially into the surrounding medium as an evanescent field. However, due to the metals' tendency to quench fluorescence at close distances, a spacer layer ranging from 5 to 20 nm separating the fluorophores from the metal surface must be used,[3] resulting in lower fluorescence enhancement efficiency as the analyte is placed in the rapidly decaying evanescent field.

Recently, one-dimensional (1D) and two-dimensional photonic crystal (PC) slabs supporting guided-mode resonances (GMRs)[4–6] have also been studied for applications in fluorescence enhancement of organic dyes[7,8] and colloidal quantum dots.[9] The GMR effect occurs when the evanescent diffracted orders of a periodic subwavelength surface structure couple to the modes of an effective high refractive index (RI) layer,[10] resulting in a strong reflection (nearly 100% efficiency) about a resonant wavelength and heightened near electric-field intensities within the structure.[11] The enhanced electric field above the PC surface follows an exponential decay[12] as in the case of metals, but since dielectric materials do not quench fluorescence, fluorophores can be placed directly in contact with the PC surface. However, in many cases, the near fields are maximized inside the high RI layer where interaction with physadsorbed fluorophores cannot take place. Therefore, a porous high RI layer would be highly desirable as a means for colocating the regions of high resonant electric-field intensity with the regions in which fluorescent dye molecules incorporate within the PC. Previously, we demonstrated that a PC design with a porous coating deposited on a dense nonporous high RI $TiO_2$ layer can enhance the fluorescent output by over 110 times[13] by both increasing the quality factor of the PC and the available surface area for biomolecule attachment. In this work, we demonstrate the design of a PC with an exclusively nanorod-structured high RI layer. We show that by allowing fluorophores to penetrate into the high RI layer where the maximum electric field is located, an enhancement of 193 times in fluorescent intensity can be achieved when compared to detecting the same analyte on the surface of an unpatterned glass slide.

The PC structure is comprised of a linear grating surface structure with a period of $\Lambda = 360$ nm and a depth of $h = 60$ nm [Fig. 1(a)] in a low RI UV cured polymer (UVCP) ($n_{\mathrm{UVCP}} = 1.46$) fabricated by a room temperature large area replica-molding process.[14] The grating is coated with a $d = 120$ nm porous $TiO_2$ layer by the glancing angle deposition technique[13,15–18] in an electron-beam deposition system (Denton Vacuum). Due to the self-shadowing effect[19,20] and limited mobility of adatoms, the porous layer is composed of isolated nanorods. Figure 1(b) shows the scanning electron microscopy (SEM) images of the fabricated PC showing nanorods uniformly coated onto the grating structure. Ellipsometry measurement shows that the nanorod $TiO_2$ layer in air has a RI of $n_{\mathrm{nanorod\ in\ air}} = 1.46$ and a porosity of 65%, assuming a linear dependence of RI on porosity.[21,22] In operation, the PC is immersed in water in order for the nanorod layer to have high enough RI contrast with respect to the substrate ($n_{\mathrm{UVCP}} = 1.46$) and superstrate ($n_{\mathrm{water}} = 1.33$) to support the GMR condition. Immersed in water, the nanorod

a)Electronic mail: bcunning@illinois.edu.

 

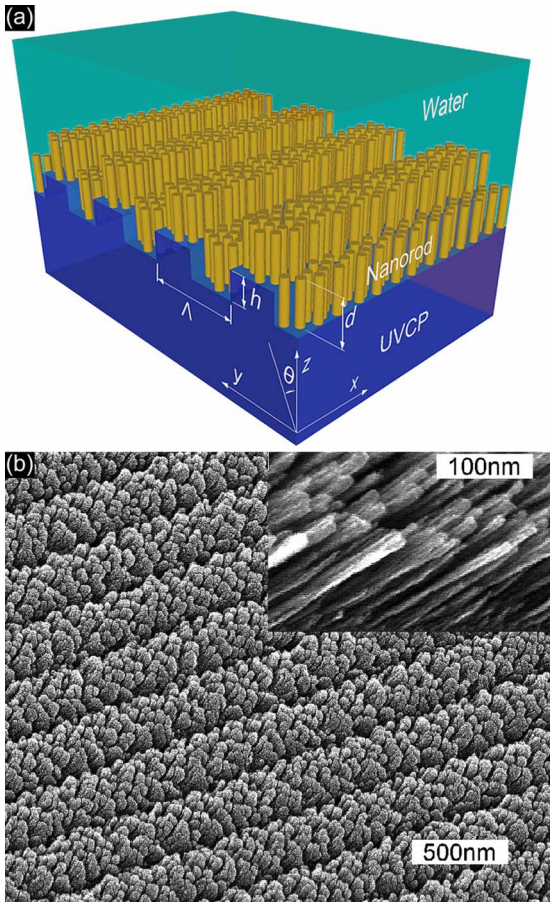


FIG. 1. (Color online) (a) Layout of the 1D PC. $\Lambda=360$ nm is the period of the grating, $h=60$ nm is the grating depth, and $d=120$ nm is the thickness of the nanorod-structured $TiO_2$ layer. (b) SEM images of the top view and side view (inset) of a fabricated PC.

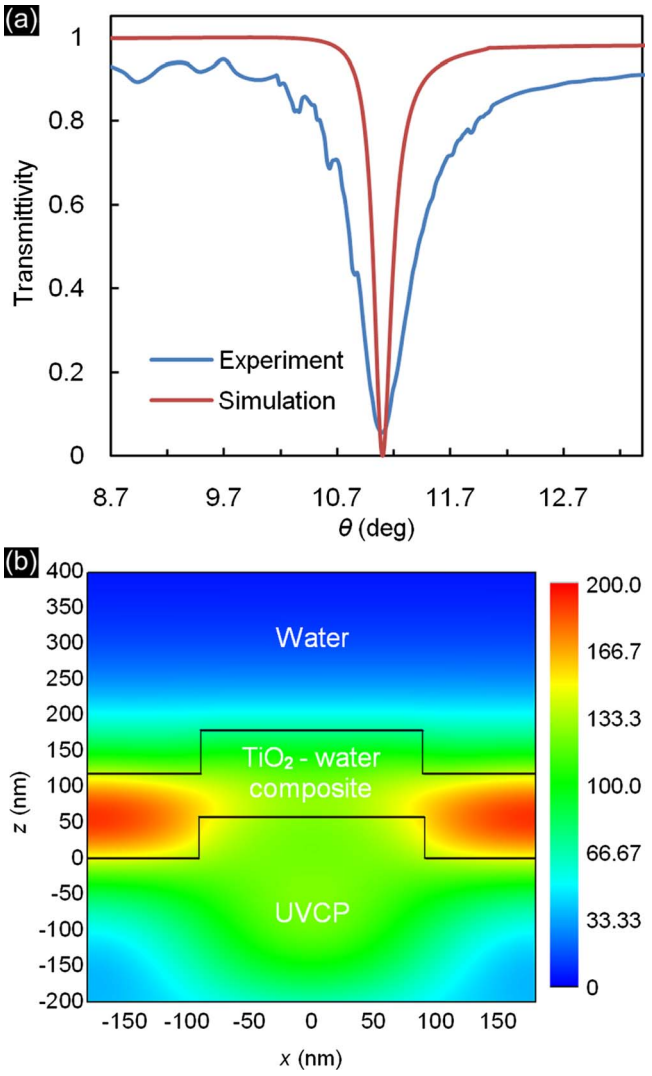


FIG. 2. (Color online) (a) Computed (red) and measured (blue) transmittivity as a function of $\theta$ for a PC immersed with water upon illumination with TE polarized light. (b) Calculated near electric-field intensity $E^2$ of the PC showing that the maximum $E^2$ is located within the high RI layer and decays into the substrate and superstrate.

layer is estimated to have a RI of $n_{\text{nanorod in water}}=1.67$, assuming a linear mixing rule of $TiO_2$:water=35:65.

Rigorous coupled-wave analysis (RCWA)[23] simulations were used to study the behavior of the PC structure upon external illumination with TE polarized light (electric field parallel to the grating lines, i.e., *x*-axis) in the *yz* plane of Fig. 1(a). The wavelength of the incident light is $\lambda=633$ nm, which corresponds to the output wavelength of a HeNe laser used to excite the fluorophore cyanine 5 (Cy5). The red curve in Fig. 2(a) shows the computed transmittivity as a function of the incident angle $\theta$ [polar angle in the *yz* plane of Fig. 1(a)] for a PC immersed in water, where the dip in the transmittivity corresponds to the resonant angle, in this case $\theta=11.1°$. Plotted as the blue curve in the same plot are the experimental data measured with a transmission setup equipped with a HeNe laser, a rotational stage, and a power meter. RCWA was also used to compute the near electric-field intensity distribution of the PC at the resonant wavelength/angle coupling condition [Fig. 2(b)]. The most intense field is located in the high RI layer of the $TiO_2$-water composite and decays into the substrate (UVCP) and superstrate (water).[24] Utilizing a modeled input electric field of unit intensity at $\lambda=633$ nm, the spatial average of $E^2$ within the nanorod layer is calculated to be 139.9. This shows that the field inside the high RI layer is much stronger as compared to $E^2=102.6$ immediately on top of the high RI layer. Therefore, through the use of a porous high RI layer, not only is the surface area of the PC greatly enhanced, but also the fluorophores may attach within a region with much stronger electric-field intensity, potentially resulting in a greater fluorescent output intensity.

To test the performance of the PC, the device was functionalized with 1% solution of a proprietary amine polymer for 26 h, followed by washing with water. A bifunctional linker glutaraldehyde ($C_5H_8O_2$, 25%, Sigma-Aldrich) was then allowed to incubate on the PC surface for 6 h and followed by a wash step. Six spots of Cy5-conjugated streptavidin (100 ng/ml, GE healthcare) were then spotted onto the PC using a pipette and allowed to incubate for 30 h, followed by a wash step. The same protocol was also applied to an unpatterned microscope slide (previously coated with 20 nm of dense nonporous $TiO_2$ by sputtering in order to terminate with the same surface material as the PC), which was used as reference for comparison. The spotted devices with a thin layer of water and a cover glass were scanned at 20 $\mu$m pixel resolution with a confocal fluorescence microarray scanner (LS 2000, Tecan) equipped with a $\lambda=633$ nm HeNe laser. The scanner is equipped with the ability to tune the angle of incident laser illumination, allowing matching of the

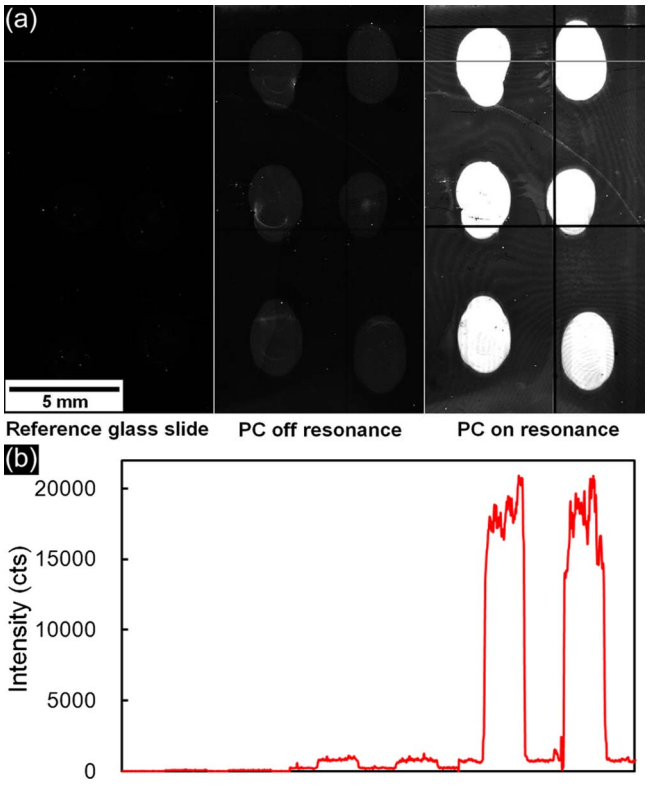


FIG. 3. (Color online) (a) Images of Cy5-labeled streptavidin spots on the reference glass slide (coated with 20 nm of compact $TiO_2$ by sputtering, scanned with $\theta=25°$) and the PC with off- ($\theta=25°$) and on- ($\theta=11.1°$) resonance conditions. (b) Fluorescent intensity plot of the horizontal line in (a).

wavelength/incident angle combination required to excite resonance in the PC. Therefore, the PC may be scanned in both on-resonance and off-resonance conditions to allow direct observation of the effects of the resonance-enhanced near fields.

Figure 3(a) shows the fluorescence scan images of the reference glass slide (scanned with $\theta=25.0°$) and the PC with off ($\theta=25.0°$) and on ($\theta=11.1°$) resonance conditions. Figure 3(b) shows a line profile of the fluorescence intensity across the images. After background subtraction, the reference glass slide has an average fluorescence intensity of 74 counts within six spots. The PC at off-resonance has an average of 705 counts, which is a 9.5 times enhancement compared to the glass slide. We believe this enhancement is primarily due to the increase in surface area by the porous nanorod structures. An average of 14 315 counts was obtained when the PC was at on-resonance, representing a 193 times enhancement when compared to the reference glass slide. The ratio of fluorescence intensity from the dyes on- and off-resonance is 20.3. This on and off ratio is ~2 times higher than a previous PC design with a dense, nonporous high RI layer, which achieved a ratio of ~10 times.[12] However, the on and off ratio from the device studied in this work is still much lower than the ~140-fold of enhancement in $E^2$ within the nanorod layer predicted by simulation. This discrepancy is due to the difference between the measured resonant linewidth [blue curve in Fig. 2(a), full width at half maximum (FWHM)=0.622°, or FWHM=4.21 nm] and the one predicted by simulation [red curve in Fig. 2(a), FWHM=0.195°, or FWHM=1.32 nm], which implies a lowered quality factor and hence less intense near fields in the real device.

In conclusion, we have fabricated a 1D PC with a nanorod-structured high RI layer that allows fluorophores to penetrate into the region with the most intense electric-field intensity. In the detection of Cy5-conjugated streptavidin, the design shows an enhancement of 193-fold in fluorescence intensity when compared to an unpatterned glass slide. The design demonstrated in this work will enable improved fluorescence detection sensitivity for a wide range of assays. In the future work, we plan to exploit this resonant surface design in the context of gene expression assays and protein biomarker assays in which an immobilized molecule is used to selectively capture a target complementary molecule from a test sample.

This work was supported by the National Science Foundation under Grant No. CBET 07–54122. Any opinions, findings, conclusions, or recommendations expressed in this material are those of the author(s) and do not necessarily reflect the views of the National Science Foundation. The authors gratefully acknowledge SRU Biosystems for providing financial support for this work. The authors also extend their gratitude to the support staff of the Micro and Nanotechnology Laboratory at the University of Illinois at Urbana-Champaign.

[1] T. Hayakawa, S. T. Selvan, and M. Nogami, Appl. Phys. Lett. **74**, 1513 (1999).
[2] Y. J. Hung, I. I. Smolyaninov, C. C. Davis, and H. C. Wu, Opt. Express **14**, 10825 (2006).
[3] O. Stranik, H. M. McEvoy, C. McDonagh, and B. D. MacCraith, Sens. Actuators B **107**, 148 (2005).
[4] S. S. Wang and R. Magnusson, Appl. Opt. **32**, 2606 (1993).
[5] S. S. Wang, R. Magnusson, J. S. Bagby, and M. G. Moharam, J. Opt. Soc. Am. A **7**, 1470 (1990).
[6] R. Magnusson and S. S. Wang, Appl. Phys. Lett. **61**, 1022 (1992).
[7] D. Neuschafer, W. Budach, C. Wanke, and S. D. Chibout, Biosens. Bioelectron. **18**, 489 (2003).
[8] P. C. Mathias, N. Ganesh, L. L. Chan, and B. T. Cunningham, Appl. Opt. **46**, 2351 (2007).
[9] N. Ganesh, W. Zhang, P. C. Mathias, E. Chow, J. A. N. T. Soares, V. Malyarchuk, A. D. Smith, and B. T. Cunningham, Nat. Nanotechnol. **2**, 515 (2007).
[10] D. Rosenblatt, A. Sharon, and A. A. Friesem, IEEE J. Quantum Electron. **33**, 2038 (1997).
[11] C. Y. Wei, S. J. Liu, D. G. Deng, J. Shen, J. D. Shao, and Z. X. Fan, Opt. Lett. **31**, 1223 (2006).
[12] N. Ganesh, P. C. Mathias, W. Zhang, and B. T. Cunningham, J. Appl. Phys. **103**, 083104 (2008).
[13] W. Zhang, N. Ganesh, P. C. Mathias, and B. T. Cunningham, "Enhanced fluorescence on a photonic crystal surface incorporating nanorod structure," Small (to be published).
[14] N. Ganesh and B. T. Cunningham, Appl. Phys. Lett. **88**, 071110 (2006).
[15] W. Zhang, N. Ganesh, I. D. Block, and B. T. Cunningham, Sens. Actuators B **131**, 279 (2008).
[16] J. G. W. v. d. Waterbeemd and G. W. v. Oosterhout, Philips Res. Rep. **22**, 375 (1967).
[17] K. Robbie, L. J. Friedrich, S. K. Dew, T. Smy, and M. J. Brett, J. Vac. Sci. Technol. A **13**, 1032 (1995).
[18] L. Abelmann and C. Lodder, Thin Solid Films **305**, 1 (1997).
[19] H. Konig and G. Helwig, Optik (Stuttgart) **6**, 111 (1950).
[20] L. Holland, J. Opt. Soc. Am. **43**, 376 (1953).
[21] D. J. Taylor, P. F. Fleig, and S. L. Hietala, Thin Solid Films **332**, 257 (1998).
[22] J. Q. Xi, J. K. Kim, E. F. Schubert, D. X. Ye, T. M. Lu, S. Y. Lin, and J. S. Juneja, Opt. Lett. **31**, 601 (2006).
[23] M. G. Moharam and T. K. Gaylord, J. Opt. Soc. Am. **71**, 811 (1981).
[24] Y. Ding and R. Magnusson, Opt. Express **12**, 1885 (2004).